

Supplementary Information for A Review of Defect Structure and Chemistry in Ceria and its Solid Solutions

Rafael Schmitt ^{1*}, Andreas Nenning ^{1,2*}, Olga Kraynis ^{3*}, Roman Korobko ^{2,3}, Anatoly I. Frenkel ⁴, Igor Lubomirsky ³, Sossina M. Haile ⁵ and Jennifer L.M. Rupp ^{1,2, 6}

1: Electrochemical Materials, Department of Materials, ETH Zurich, Switzerland

2: Electrochemical Materials, Department of Materials Science and Engineering, Massachusetts Institute of Technology, Cambridge, MA, 02139, USA

3: Dept. Materials and Interfaces, Weizmann Institute of Science, Rehovot 76100, Israel

4: Department of Materials Science and Chemical Engineering, Stony Brook University, Stony Brook, NY 11794, USA

5: Materials Science and Engineering, Northwestern University, Evanston, IL, USA

6: Electrochemical Materials, Department of Electrical Engineering & Computer Science, Massachusetts Institute of Technology, Cambridge, MA, 02139, USA

** Shared first-co-authorship, these authors have equally contributed to this manuscript.*

Corresponding author: jrupp@mit.edu

1. Supplementary Information for Section 3

The figures in Section 3 of the manuscript were prepared by an extensive and thorough literature search. In the following tables, the values and references for all plotted data points are summarized. The error in the last significant digit is in parentheses (*e.g.* 2.30 ± 0.01 is given as $2.30(1)$).

1.1. Data for Figure 9 – first and second shell distance comparison

Table S1: First and second shell distances derived using EXAFS for doped ceria materials at 10 and 20 mol% doping. Data for Sm, Er and Yb doped ceria were taken from: Giannici *et al.*^{1,2}. Data for Gd, Y and La doped ceria were taken from: Deguchi *et al.*⁶.

Giannici <i>et al.</i>				
x mol%	Sm doped ceria (Å)			
	<i>Ce-O</i>	<i>Sm-O</i>	<i>Ce-Ce</i>	<i>Sm-Ce</i>
10	2.30(1)	2.42 (1)	3.81(1)	3.77(1)
20	2.28(1)	2.40 (1)	3.81(1)	3.79(1)
x mol%	Er doped ceria (Å)			
	<i>Ce-O</i>	<i>Er-O</i>	<i>Ce-Ce</i>	<i>Er-Ce</i>
10	2.29(1)	2.30(2)	3.81(1)	3.79(1)
20	2.29(1)	2.30(1)	3.80(1)	3.76(1)
x mol%	Yb doped ceria (Å)			
	<i>Ce-O</i>	<i>Yb-O</i>	<i>Ce-Ce</i>	<i>Yb-Ce</i>
10	2.30(1)	2.30(1)	3.81(1)	3.77(1)
20	2.28(1)	2.28(1)	3.81(1)	3.75(1)

Deguchi <i>et al.</i>				
x mol%	Gd doped ceria (Å)			
	<i>Ce-O</i>	<i>Gd-O</i>	<i>Ce-Ce</i>	<i>Gd-Ce</i>
10	2.340(6)	2.383(6)	3.82(1)	3.82(3)
20	2.333(6)	2.377(6)	3.82(1)	3.80(3)
x mol%	Y doped ceria (Å)			
	<i>Ce-O</i>	<i>Y-O</i>	<i>Ce-Ce</i>	<i>Y-Ce</i>
10	2.344(6)	2.323(6)	3.82(1)	3.79(3)
20	2.337(6)	2.319(6)	3.82(1)	3.77(3)
x mol%	La doped ceria (Å)			
	<i>Ce-O</i>	<i>La-O</i>	<i>Ce-Ce</i>	<i>La-Ce</i>
10	2.343(6)	2.465(6)	3.89(1)	3.85(3)
20	2.334(6)	2.471(6)	3.90(1)	3.86(3)

1.2. Data for Figure 10, calculated Cat-Vo distances

Table S2: The EXAFS first shell distances (R_{EXAFS}^{Ce-O} and R_{EXAFS}^{Do-O}) together with XRD lattice parameters a .

The data is used to estimate the first shell distance around the vacancy site $R_{calculated}^{Cat-V_o}$. Data for Gd was obtained from references ³⁻⁵. Data for Sm was obtained from references ^{1, 2}.

Gd doped	x	R_{EXAFS}^{Ce-O} (Å)	R_{EXAFS}^{Gd-O} (Å)	a (Å)	$R_{Calculated}^{Cat-V_o}$ (Å)
Li <i>et al.</i> ⁵	0.05(1)	2.33(1)	2.34(1)	5.419(1)	3.6(8)
	0.10(1)	2.34(1)	2.33(1)	5.421(1)	2.7(4)
Kossov <i>et al.</i> ⁴	0.05(1)	2.325(6)	2.36(1)	5.412(3)	3.6(8)
	0.10(1)	2.319(6)	2.364(7)	5.417(3)	3.2(4)
	0.15(1)	2.315(5)	2.35(2)	5.421(3)	3.1(2)
	0.20(1)	2.314(6)	2.35(1)	5.426(3)	2.9(2)
Kossov <i>et al.</i> ³	0.20(1)	2.325(8)	2.375(8)	5.425(1)	2.6(1)
Sm doped	x	R_{EXAFS}^{Ce-O} (Å)	R_{EXAFS}^{Sm-O} (Å)	a (Å)	$R_{Calculated}^{Cat-V_o}$ (Å)
Giannici <i>et al.</i> ¹	0.10(1)	2.30 (1)	2.42 (1)	5.4234(1)	3.9(4)
	0.20(1)	2.28 (1)	2.40 (1)	5.4322(1)	3.1(2)
	0.3(1)	2.26 (1)	2.39 (1)	5.4421(1)	3.0(1)
Nitani <i>et al.</i> ²	0.20(1)	2.339(1)	2.407(1)	5.435(1)	2.4(2)
	0.30(1)	2.335(1)	2.403(1)	5.440(1)	2.4(1)

1.3. Data for Figure 12: local (EXAFS) vs. average (XRD) trends of Cat-An as a function of doping fraction

The following tables (Table S3-Table S12) contain first shell distances derived using EXAFS for *Ce-O* and *Do-O*, as well as lattice parameters a and *Cat-An* distances derived from them (using Eq. 21 in the main text). The slope "Cat-An vs. x (Å/mol%)" was extracted from linear regression fits for each series and is presented in the last row of each table. If several data sets are available for the same interatomic distance, e.g. four slopes for *Ce-O* of Gd-doped ceria in Table S3, the statistical average is given in the summary Table S13. The same applies to *Do-O* and R_{XRD}^{Cat-An} series where several data sets are available. The summary Table S13 provides the data sets for Figure 12 in the main text.

Table S3: EXAFS first shell distances for Gd doped ceria, obtained from references^{4, 6-8}. A question mark (?) indicates error bars were unavailable for that data.

Gd doped ceria - EXAFS literature data								
<i>x mol%</i>	Ce-O(Å)				Gd-O(Å)			
	Ohashi (1998)	Yamazaki (2000)	Deguchi (2005)	Kossoy (2013)	Ohashi (1998)	Yamazaki (2000)	Deguchi (2005)	Kossoy (2013)
5	2.34(?)		2.343(6)	2.325(6)			2.382(6)	2.36(1)
10	2.33(?)	2.33(?)	2.340(6)	2.319(6)	2.38(?)	2.41(?)	2.383(6)	2.364(7)
15				2.315(5)				2.35(2)
20	2.32(?)	2.32(?)	2.333(6)	2.314(6)	2.37(?)	2.38(?)	2.377(6)	2.35(1)
25				2.29(1)				2.350(5)
30	2.31(?)	2.30(?)	2.320(6)		2.35(?)	2.36(?)	2.370(6)	
<i>Cat-An</i> vs. <i>x</i> (Å/mol%)	- (1.20 ± 0.06)	- (1.5 ± 0.03)	- (0.9 ± 0.1)	- (1.5 ± 0.5)	- (1.4 ± 0.06)	- (2.6 ± 0.3)	- (0.5 ± 0.1)	- (0.9 ± 0.4)
	E-3	E-3	E-3	E-3	E-3	E-3	E-3	E-3

Table S4: XRD lattice parameter data and derived Cat-An distances for Gd doped ceria. Obtained from references^{4, 9, 10}.

Gd -XRD literature data								
<i>x mol%</i>	<i>a</i> (Å)			$R^{Cat-An}_{XRD} = \frac{\sqrt{3}}{4} \cdot a$ (Å)				
	Yavo (2016)	Hong (1995)	Kossoy (2013)	Yavo (2016)	Hong (1995)	Kossoy (2013)		
0	5.412(3)				2.343(1)			
2	5.414(3)				2.344(1)			
5	5.416(3)	5.412(3)		2.345(1)		2.343(1)		
6	5.415(3)				2.345(1)			
9	5.417(3)				2.345(1)			
10	5.418(3)	5.417(3)		2.346(1)		2.346(1)		
13	5.422(3)				2.348(1)			
15		5.421(3)				2.347(1)		
17		5.427(3)			2.350(1)			
20	5.425(3)	5.432(3)	5.426(3)	2.349(1)	2.352(1)	2.349(1)		
23		5.432(3)			2.352(1)			
<i>Cat-An</i> vs. <i>x</i> (Å/mol%)				(0.27 ± 0.03)	(0.42 ± 0.03)	(0.41 ± 0.01)		
				E-3	E-3	E-3		

Table S5: XRD lattice parameter data a (\AA) for Sm doped ceria and derived first shell distances R_{XRD}^{Cat-O} obtained from references^{1, 9, 11}. EXAFS first shell distances for Sm doped ceria obtained from references^{1, 8}.

Sm- XRD literature data						Sm- EXAFS literature data			
x <i>mol%</i>	a (\AA)			$R_{XRD}^{Cat-An} = \frac{\sqrt{3}}{4} \cdot a$ (\AA)			$Ce-O$ (\AA)		$Sm-O$ (\AA)
	Coduri (2018)	Hong (1995)	Giannici (2014)	Coduri (2018)	Hong (1995)	Giannici (2014)	Giannici (2014)	Yamazaki (2000)	Giannici (2014)
0	5.4072(1)	5.412(3)		2.3413(1)	2.344(1)				
6		5.423(3)			2.348(1)				
9		5.429(3)			2.351(1)				
10			5.4234(1)			2.3488(1)	2.30 (1)	2.33 (?)	2.42 (1)
13	5.4214(1)	5.431(3)		2.3475(1)	2.352(1)				
17		5.432(3)			2.352(1)				
20		5.438(3)	5.4322(1)		2.355(1)	2.3528(1)	2.28 (1)	2.31 (?)	2.40 (1)
23		5.437(3)			2.354(1)				
25	5.4350(1)			2.3534(1)					
30	5.4413(1)		5.4421(1)	2.3561(1)		2.3575(1)	2.26 (1)	2.30 (?)	2.39 (1)
<i>Cat-An vs. x</i> ($\text{\AA}/\text{mol\%}$)			(0.48±0.06) E-3	(0.46±0.06) E-3	(0.43±0.02) E-3	- E-3	- E-3	- E-3	- E-3

Table S6: XRD lattice parameter data a (\AA) for Y doped ceria and derived first shell distances R_{XRD}^{Cat-O} obtained from reference¹². EXAFS first shell distances for Y doped ceria obtained from references^{6, 8}.

Y- XRD literature data			Y- EXAFS literature data			
x <i>mol%</i>	a (\AA)	$R_{XRD}^{Cat-An} = \frac{\sqrt{3}}{4} \cdot a$ (\AA)	R_{EXAFS}^{Ce-O} (\AA)		R_{EXAFS}^{Y-O} (\AA)	
	Coduri (2013)	Coduri (2013)	Deguchi (2005)	Yamazaki (2000)	Deguchi (2005)	Yamazaki (2000)
0	5.4077(1)	2.3416(1)				
5			2.345(6)	2.34(?)	2.329(6)	
10	5.4060(1)	2.3409(1)	2.344(6)	2.34(?)	2.323(6)	2.32(?)
15			2.340(6)	2.33(?)	2.322(6)	2.32(?)
20			2.337(6)	2.32(?)	2.319(6)	2.31(?)
25	5.4032(1)	2.3397(1)		2.32(?)		2.31(?)
30			2.329(6)	2.31(?)	2.316(6)	2.31(?)
<i>Cat-An vs. x</i> ($\text{\AA}/\text{mol\%}$)		-(0.077±0.002) E-3	-(0.67±0.06) E-3	-(1.47±0.08) E-3	-(0.46±0.07) E-3	-(0.42±0.05) E-3

Table S7: XRD lattice parameter data a (\AA) for Er doped ceria and derived first shell distances R_{XRD}^{Cat-O} obtained from references^{1, 9}. EXAFS first shell distances for Er doped ceria obtained from reference¹.

Er- XRD literature data				Er- EXAFS literature data	
$x \text{ mol\%}$	a (\AA)		$R_{XRD}^{Cat-An} = \frac{\sqrt{3}}{4} \cdot a$ (\AA)	R_{EXAFS}^{Ce-O} (\AA)	R_{EXAFS}^{Er-O} (\AA)
	Hong (1995)	Giannici (2014)	Giannici (2014)	Giannici (2014)	Giannici (2014)
0	5.412(3)		2.343(1)		
2	5.411(3)		2.343(1)		
6	5.409(3)		2.342(1)		
9	5.409(3)		2.342(1)		
10		5.4051(1)		2.3405(1)	2.29(1)
13	5.409(3)	--	2.342(1)	--	
17	5.406(3)		2.341(1)		
20	5.405(3)	5.3999(1)	2.341(1)	2.3382(1)	2.29(1)
23	5.405(3)		2.340(1)		2.30(1)
30		5.3896(1)		2.3338(1)	2.28(1)
<i>Cat-An vs. x</i> (\AA/mol\%)			-(0.13±0.01) E-3	-(0.33±0.06) E-3	-(0.5±0.3) E-3
					0

Table S8: XRD lattice parameter data a (\AA) for Yb doped ceria and derived first shell distances R_{XRD}^{Cat-O} obtained from references^{1, 9}. EXAFS first shell distances for Y doped ceria obtained from references^{1, 8}.

Yb- XRD literature data				Yb- EXAFS literature data			
$x \text{ mol\%}$	a (\AA)		$R_{XRD}^{Cat-An} = \frac{\sqrt{3}}{4} \cdot a$ (\AA)	R_{EXAFS}^{Ce-O} (\AA)	R_{EXAFS}^{Yb-O} (\AA)		
	Hong (1995)	Giannici (2014)	Hong (1995)	Giannici (2014)	Giannici (2014)	Yamazaki (2000)	Giannici (2014)
0	5.412(3)		2.344(1)				
2	5.411(3)		2.343(1)				
6	5.407(3)		2.341(1)				
9	5.406(3)		2.341(1)				
10		5.3993(1)		2.3380(1)	2.30(1)	2.33?	2.30(1)
13	5.403(3)		2.339(1)	--			
17	5.398(3)		2.337(1)				
20	5.394(3)	5.3875(1)	2.335(1)	2.3329(1)	2.28(1)	2.32?	2.28(1)
23	5.388(3)		2.333(1)				
30		5.3762(1)		2.3280(1)	2.28(1)	2.30(?)	2.27(1)
<i>Cat-An vs. x</i> (\AA/mol\%)			-(0.43±0.03) E-3	0.500±0.006 E-3	-(1.0±0.6) E-3	-(1.2±0.1) E-3	-(1.5±0.3) E-3

Table S9: XRD lattice parameter data a (\AA) for Nd doped ceria and derived first shell distances R_{XRD}^{Cat-An} obtained from references ^{9, 13}. EXAFS first shell distances for Nd doped ceria obtained from reference ⁸.

Nd- XRD literature data				Nd- EXAFS literature data	
$x \text{ mol\%}$	a (\AA)		$R_{XRD}^{Cat-An} = \frac{\sqrt{3}}{4} \cdot a$ (\AA)	$Ce-O$ (\AA)	
	Hong (1995)	Stephens (2006)	Hong (1995)	Stephens (2006)	Yamazaki (2000)
0	5.412(3)	5.411(5)	2.343(1)	2.343(2)	
2	5.415(3)		2.345(1)		
3		5.425(5)		2.349(2)	
5		5.429(5)		2.351(2)	
6	5.426(3)		2.350(1)		
9	5.432(3)		2.352(1)		
10		5.436(5)		2.354(2)	2.33(?)
13	5.437(3)		2.354(1)		
17	5.440(3)		2.356(1)		
20	5.447(3)	5.444(5)	2.358(1)	2.357(2)	2.31(?)
23	5.451(3)		2.360(1)		2.29(?)
<i>Cat-An vs. x</i> ($\text{\AA}/\text{mol\%}$)			(0.72±0.04) E-3	(0.6±0.1) E-3	-(1.7±0.2) E-3

Table S10: XRD lattice parameter data a (\AA) for La doped ceria and derived first shell distances R_{XRD}^{Cat-An} obtained from references ^{9, 14}. EXAFS first shell distances for La doped ceria obtained from reference ⁶.

La- XRD literature data				La- EXAFS literature data		
$x \text{ mol\%}$	a (\AA)		$R_{XRD}^{Cat-An} = \frac{\sqrt{3}}{4} \cdot a$ (\AA)	$Ce-O$ (\AA)	$La-O$ (\AA)	
	Hong	McBride	Hong	McBride	Deguchi	Deguchi
0	5.412(3)	5.4110(5)	2.343(1)	2.3430(2)		
2	5.419(3)		2.346(1)			
5		5.4272(5)		2.3500(2)	2.347(6)	2.460(6)
6	5.432(3)		2.352(1)			
9	5.443(3)		2.357(1)			
10		5.4430(5)		2.3569(2)	2.344(6)	2.465(6)
13	5.455(3)		2.362(1)			
15					2.338(6)	2.468(6)
17	5.458(3)		2.364(1)			
20	5.462(3)	5.4750(5)	2.365(1)	2.3707(2)	2.334(6)	2.471(6)
23	5.466(3)		2.367(1)			
30					2.323(6)	
<i>Cat-An vs. x</i> ($\text{\AA}/\text{mol\%}$)			(1.04±0.09)	(1.39±0.01)	-(0.96±0.05)	(0.72±0.06)

Table S11: XRD lattice parameter data a (\AA) for Sc doped ceria and derived first shell distances R_{XRD}^{Cat-An} obtained from reference ⁵. EXAFS first shell distances for Sc doped ceria obtained from reference ⁸.

	Sc- XRD literature data		Sc- EXAFS literature data
$x \text{ mol\%}$	a (\AA)	$R_{XRD}^{Cat-An} = \frac{\sqrt{3}}{4} \cdot a$ (\AA)	$Ce-O$ (\AA)
	Li (1991)	Li (1991)	Yamazaki (2000)
0	5.410(?)	2.343(?)	
1	5.405(?)	2.340(?)	
5	5.387(?)	2.333(?)	
9	5.373(?)	2.327(?)	
10			2.33(?)
20			2.34(?)
30			2.34(?)
<i>Cat-An vs. x</i> (\AA/mol\%)		-(1.6±0.1) E-3	(0.2±0.1) E-3

Table S12: XRD lattice parameter data a (\AA) for In, Lu, Dy, Tb and Eu doped ceria and derived first shell distances R_{XRD}^{Cat-An} obtained from references ^{5, 9, 14, 15}.

XRD literature data for dopants with no parallel EXAFS data					
In ref. ⁵			Lu ref. ¹⁵		
x%	a (\AA)	$R_{XRD}^{Cat-An} = \frac{\sqrt{3}}{4} \cdot a$ (\AA)	x%	a (\AA)	$R_{XRD}^{Cat-An} = \frac{\sqrt{3}}{4} \cdot a$ (\AA)
Li (1991)	Li (1991)		Varenik (2018)	Varenik (2018)	
0	5.410(?)	2.343(?)	0	5.4135(3)	2.3441(1)
1	5.408(?)	2.342(?)	1		
2			2	5.4107(3)	2.3429(1)
4			4	5.4085(4)	2.3419(2)
5	5.399(?)	2.338(?)	5		
8			8	5.4045(3)	2.3402(1)
13			13	5.3995(4)	2.3381(2)
17			17	5.3958(6)	2.3364(3)
<i>Cat-An vs. x</i> ($\text{\AA}/\%$)		- $(1.04 \pm 0.04)\text{E-3}$	<i>Cat-An</i> (\AA) <i>vs. x</i> (%)		- $(0.45 \pm 0.01)\text{E-3}$
Dy ref. ⁹			Tb ref. ¹⁴		
x%	a (\AA)	$R_{XRD}^{Cat-An} = \frac{\sqrt{3}}{4} \cdot a$ (\AA)	x%	a (\AA)	$R_{XRD}^{Cat-An} = \frac{\sqrt{3}}{4} \cdot a$ (\AA)
Hong (1995)	Hong (1995)		McBride (1994)	McBride (1994)	
0	5.412(3)	2.344(1)	0	5.4110(5)	2.3430(2)
4			4	5.4093(5)	2.3423(2)
6	5.413(3)	2.344(1)	6		
9	5.414(3)	2.344(1)	9	5.4089(5)	2.3421(2)
13	5.412(3)	2.344(1)	13		
18			18	5.4084(5)	2.3419(2)
20	5.415(3)	2.345(1)	20		
23	5.410(3)	2.342(1)	23		
<i>Cat-An vs. x</i> ($\text{\AA}/\%$)		- $(0.02 \pm 0.04)\text{E-3}$	<i>Cat-An</i> (\AA) <i>vs. x</i> (%)		- $(0.026 \pm 0.004)\text{E-3}$
Eu ref. ¹⁴					
x%	Lattice parameters [\AA]	$R_{XRD}^{Cat-An} = \frac{\sqrt{3}}{4} \cdot a$ [\AA]			
McBride (1994)	McBride (1994)				
0	5.4110(5)	2.3430(2)			
5	5.4159(5)	2.3451(2)			
10	5.4241(5)	2.3487(2)			
19	5.4266(5)	2.3498(2)			
<i>Cat-An vs. x</i> ($\text{\AA}/\%$)		$(0.3 \pm 0.1)\text{E-3}$			

Table S13: Summary table containing Ce-O (EXAFS), Do-O (EXAFS) and Cat-An (XRD) vs. x mol% slopes, as presented in Figure 12 of the main text. The slope values in (Å/%) are statistical averages of all relevant data summarized in Table S3-Table S12 above.

Shannon Ionic Radius - VIII (pm)	Dopant in ceria	EXAFS		XRD Cat-An vs. x (Å/%)
		Ce-O vs. x (Å/%)	Do-O vs. x (Å/%)	
87	Sc	0.2±0.1	--	-1.6±0.1
92	In			-0.96±0.05
97.7	Lu			-0.45±0.01
98.5	Yb	-1.1±0.1	-1.5±0.3	-0.46±0.04
100.4	Er	-0.5±0.3	0	-0.23±0.01
102	Y	-1.1±0.6	-0.4±0.03	-0.077±0.002
102.7	Dy			-0.02±0.04
104	Tb			-0.026±0.004
105	Gd	-1.3±0.3	-1.3±0.9	0.46±0.02
106.6	Eu			0.3±0.1
108	Sm	-1.7±0.4	-1.5±0.3	0.46±0.02
111	Nd	-1.7±0.2	--	0.67±0.07
116	La	-1.0±0.5	0.5±0.1	1.2±0.2

2. Supplementary Information for Section 4

2.1. Materials and Methods

2.1.1. Ceramic Pellet Fabrication

The ceramic pellets of CeO_2 and $\text{Ce}_{0.8}\text{RE}_{0.2}\text{O}_{1.9}$ ($\text{RE}=\text{Y}, \text{Er}, \text{Gd}, \text{La}$) were prepared by solid state synthesis, mixing stoichiometric amounts of CeO_2 (99.9%, Cerac specialty inorganics), $\text{Ce}_{0.9}\text{Gd}_{0.1}\text{O}_{1.95}$ (99.9%, Praxair), $\text{Ce}_{0.9}\text{Gd}_{0.2}\text{O}_{1.9}$ (99.9%, Praxair) and Gd_2O_3 (99.99%, Alfa Aesar). The powders were thoroughly mixed, pressed uniaxially at 5.3 MPa for 2 minutes and subsequently isostatically at 350 MPa for 2 minutes and sintered at 1600°C for 24 h with heating and cooling rates of $\pm 5^\circ\text{C}/\text{min}$ (Nabertherm LHT08/17, Germany).

2.1.2. X-Ray Diffractometry

The structural phase of the ceramic pellets was measured by X-ray diffraction with Bragg-Brentano geometry (Bruker D8) at Cu K_α wavelength. Rietveld refinement was used to determine the lattice constant of the doped ceria pellets. The $Fm-3m$ structure was used for refinement with the Ce atoms on the $4a$ sites and the oxygen on the $8c$ sites and a starting lattice parameter of 5.40 Å.

2.1.3. Raman Spectroscopy

The Raman spectra were recorded using a confocal WITec alpha300R Raman microscope instrument (WITec, Germany) equipped with 457 nm, 532 nm, and 633 nm wavelength lasers for excitation and a spectral resolution of 0.4 cm^{-1} . 457 nm laser wavelength is used unless otherwise noticed. Fitting was done by OriginPro 9.0G using a Lorentzian function for the F_{2g} and Δ_{480} modes and Gaussian for all others. A linear background was subtracted from the measured data.

High temperature Raman spectra were acquired on a CeO_2 pellet mounted on a silver Linkam TMS600 button heater. The temperature difference between button heater and pellet was calibrated with help of a reference pellet that had a PT1000 temperature sensor.

2.2. Full Raman Spectra of Rare-Earth-Doped Ceria

The Raman spectra of the rare-earth doping series of ceria are shown in Figure S1 up to 700 cm^{-1} .

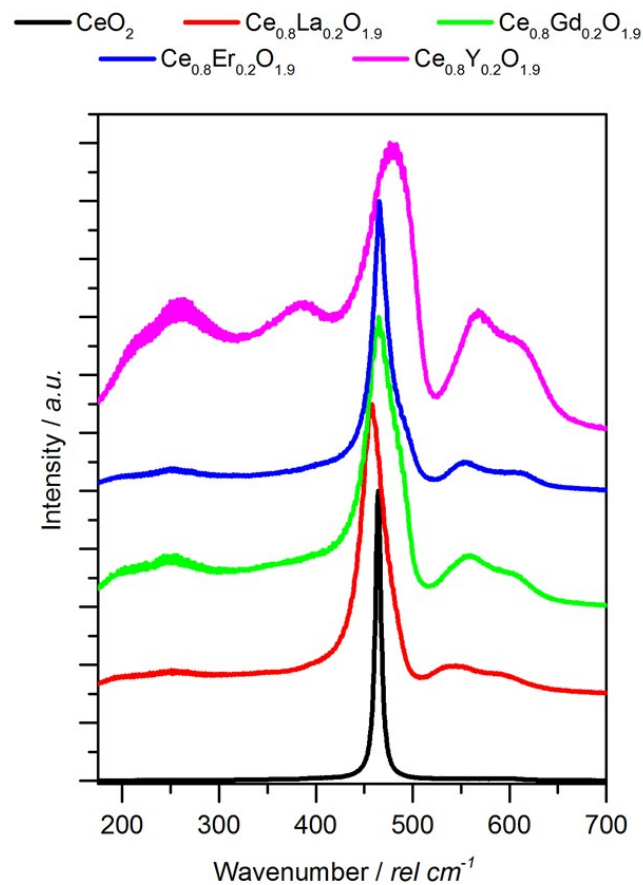


Figure S1: Raman spectra of 20 mol% rare-earth doped CeO_2 with La, Gd, Er, and Y.

2.3. Fluorescence in Erbia-Doped Ceria

The analysis of Raman spectra and the identification of Raman bands using a single excitation wavelength can lead to ambiguous interpretation because of the possible presence of fluorescence emissions in the spectrum, a challenge that is also known in other compounds, such as zirconia.¹⁶

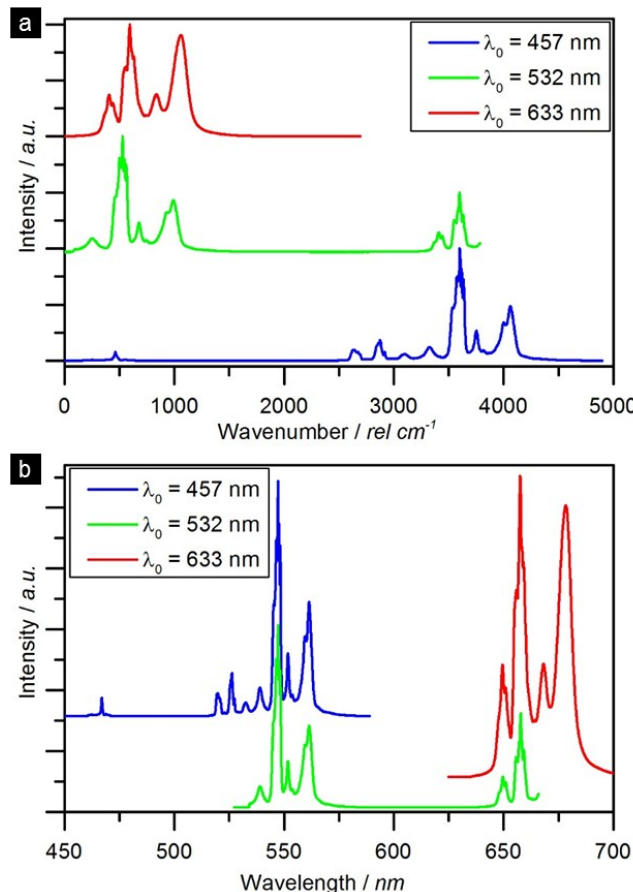


Figure S2: Raman spectra of 20 mol% $\text{ErO}_{1.5}$ doped ceria pellets measured with different excitation wavelengths of 457 nm, 532.3 nm, and 633 nm with a) relative wavenumber and b) absolute wavelength representation of the same data.

We illustrate the importance of using multiple excitation wavelengths in the example of 20 mol% $\text{ErO}_{1.5}$ -doped ceria that was characterized by their Raman response with wavelengths of 457 nm, 532 nm, and 633 nm lasers.

In Figure S1a, the recorded spectra are presented in relative wavenumbers (cm^{-1}) with respect to the source energy (defined at 0 cm^{-1}). Comparison of the spectra shows large differences in the peak positions and shapes for the different excitation wavelengths. This result is contrary to the theory of Raman scattering where a given Raman mode is expected to appear at the same relative wavenumber irrespective of the excitation energy. If in contrast, the data is displayed as a function of wavelength, the peaks measured with the different excitation wavelengths overlap, Figure S2b.

These results show unambiguously the presence of fluorescence in the recorded spectra on the example of erbia-doped ceria, in which the emission lines coincide regardless of the excitation wavelength. Similar results were obtained in pure erbia,¹⁷ and the position of the emission lines can be related to electronic transitions within the Er³⁺ ion.¹⁸ Michael *et al.* revealed that upconversion mechanisms within Er³⁺ are responsible for the fluorescence that is most intense around 550 nm and 670 nm,¹⁸ which coincides with the region investigated with the green and the red laser respectively.

A further indication for fluorescence is the strong intensity of the spectral bands that overlay the Raman modes (due to a larger cross-section for the fluorescence process). This is evident in the Raman spectrum measured with the blue laser, Figure S2b, where the F_{2g} ceria peak is barely visible at 465 cm⁻¹ compared to the strong fluorescence lines around 3500 cm⁻¹. This leads to the saturation of the detector when using the standard measurement parameters for Raman spectroscopy of undoped ceria.

These results exemplify how fluorescence can act as a major obstacle for Raman spectroscopy on oxides and can be identified using various laser wavelengths. It illustrates the paramount importance of comparing the Raman spectra recorded using multiple excitation wavelengths to account for the possible occurrence of fluorescence and discussion towards Raman modes of the oxide itself.

2.4. Data for Figure 19 in the manuscript (F_{2g} vs doping)

Table S14: Physical parameters of the elements employed in the solid solutions for analysis of the origin of the defect bands. The ionic radius in sixfold and eightfold coordination is taken from Shannon.¹⁹ The lattice parameter was determined from 20 mol% REO_{1.5}-doped CeO₂ pellets using XRD and Rietveld refinement.

Dopant	Atomic mass (u)	Ionic radius (Å)		Lattice parameter for 20% doping (Å)
		VI	VIII	
Y ³⁺	88.9	0.90	1.02	5.3976
Er ³⁺	167.3	0.89	1.00	5.4025
Ce ⁴⁺	140.1	0.87	0.97	5.4106
Gd ³⁺	157.3	0.94	1.05	5.4278
La ³⁺	138.9	1.03	1.16	5.4563

3. References

1. F. Giannici, G. Gregori, C. Aliotta, A. Longo, J. Maier and A. Martorana, *Chemistry of Materials*, 2014, **26**, 5994-6006.
2. H. Nitani, T. Nakagawa, M. Yamanouchi, T. Osuki, M. Yuya and T. A. Yamamoto, *Materials Letters*, 2004, **58**, 2076-2081.
3. A. Kossoy, A. I. Frenkel, Q. Wang, E. Wachtel and I. Lubomirsky, *Advanced Materials*, 2010, **22**, 1659-1662.
4. A. Kossoy, Q. Wang, R. Korobko, V. Grover, Y. Feldman, E. Wachtel, A. K. Tyagi, A. I. Frenkel and I. Lubomirsky, *Physical Review B*, 2013, **87**, 054101.
5. P. Li, I. W. Chen, J. E. Pennerhahn and T. Y. Tien, *J Am Ceram Soc*, 1991, **74**, 958-967.
6. H. Deguchi, H. Yoshida, T. Inagaki and M. Horiuchi, *Solid State Ionics*, 2005, **176**, 1817-1825.
7. T. Ohashi, S. Yamazaki, T. Tokunaga, Y. Arita, T. Matsui, T. Harami and K. Kobayashi, *Solid State Ionics*, 1998, **113**, 559-564.
8. S. Yamazaki, T. Matsui, T. Ohashi and Y. Arita, *Solid State Ionics*, 2000, **136**, 913-920.
9. S. J. Hong and A. V. Virkar, *J Am Ceram Soc*, 1995, **78**, 433-439.
10. N. Yavo, D. Noiman, E. Wachtel, S. Kim, Y. Feldman, I. Lubomirsky and O. Yeheskel, *Scripta Materialia*, 2016, **123**, 86-89.
11. M. Coduri, P. Masala, M. Allieta, I. Peral, M. Brunelli, C. A. Biffi and M. Scavini, *Inorganic chemistry*, 2017, **57**, 879-891.
12. M. Coduri, M. Scavini, M. Allieta, M. Brunelli and C. Ferrero, *Chemistry of Materials*, 2013, **25**, 4278-4289.
13. I. E. Stephens and J. A. Kilner, *Solid State Ionics*, 2006, **177**, 669-676.
14. J. McBride, K. Hass, B. Poindexter and W. Weber, *Journal of Applied Physics*, 1994, **76**, 2435-2441.
15. M. Varenik, X.-D. Zhang, G. Leitus, N. Yavo, R. Carmieli, E. Wachtel, X. Guo and I. Lubomirsky, *Physical Chemistry Chemical Physics*, 2018, **20**, 27019-27024.
16. J. Joo, T. Yu, Y. W. Kim, H. M. Park, F. Wu, J. Z. Zhang and T. Hyeon, *Journal of the American Chemical Society*, 2003, **125**, 6553-6557.
17. J. Cui and G. A. Hope, *Journal of Spectroscopy*, 2015, **2015**, 8.
18. C. P. Michael, H. B. Yuen, V. A. Sabnis, T. J. Johnson, R. Sewell, R. Smith, A. Jamora, A. Clark, S. Semans, P. B. Atanackovic and O. Painter, *Opt. Express*, 2008, **16**, 19649-19666.
19. R. Shannon, *Acta Crystallographica Section A*, 1976, **32**, 751-767.